Available online at www.sciencedirect.com
ScienceDirect
Ceramics International 38 (2012) 1003–1010
CERAMICS INTERNATIONAL
www.elsevier.com/locate/ceramint

Hydroxyapatite formation by solvothermal treatment of α-tricalcium phosphate with water–ethanol solution

Tomoyo Goto *, Ill Yong Kim, Koichi Kikuta, Chikara Ohtsuki

Graduate School of Engineering, Nagoya University, Furo-cho, Chikusa-ku, Nagoya 464-8603, Japan

Received 9 July 2011; received in revised form 9 August 2011; accepted 10 August 2011
Available online 17 August 2011

Abstract

We investigated hydroxyapatite (HAp) formation from alpha-tricalcium phosphate (α-TCP) under solvothermal conditions using water–ethanol solution. The rate of HAp formation decreased with increasing ethanol fraction in the solution. Needle-like HAp was formed with a small amount of beta-tricalcium phosphate after solvothermal treatment for 3 h in solutions with water/ethanol volume ratios of 5/15 and 10/10. In the solution with water/ethanol volume ratio of 5/15, needle-like HAp formed with a small amount of dicalcium phosphate anhydrous (DCPA) at 12 h, and the amount of DCPA increased with increasing treatment period. The aspect ratio of the HAp crystals that formed increased with increasing ethanol fraction in the solution. The fraction of ethanol in the solution during the solvothermal processing affects not only the rate of transformation of α-TCP into HAp, but also the morphology of the HAp that is formed.

Keywords: B. X-ray methods; D. Apatite; E. Biomedical applications; Solvothermal processing

1. Introduction

Hydroxyapatite (HAp; $Ca_{10}(PO_4)_6(OH)_2$) has been used as a bone substitute in the treatment of bone defects, because it shows good osteoconductivity [1]. In addition, HAp has been studied as a chromatography column filler [2–5] and carrier for drug delivery [6,7]. The protein adsorption characteristics of HAp crystals depend on their morphology, with different crystal faces having different characteristics. HAp is a hexagonal crystal, which has two types of crystal planes, *a*-face and *c*-face. The *a*-face is positively charged due to calcium ions, while the *c*-face is negatively charged due to oxygen atoms belonging to phosphate ions. Different types of proteins, such as basic and acidic proteins, adsorb selectively on the crystal planes of HAp [4,5]. Furthermore, crystal morphology and size affect solubility, specific surface area and mechanical strength. Material characteristics derived from crystal morphology and size is also important for cellular activity and biodegradability under body environment. Relationship between various morphologies of HAp nanocrystal and cellular behavior in vitro were reported [8,9]. In addition, the biological response of calcium-deficient HAp consisting of rod-shaped particles showed higher capability of degradation by osteoclastic cells, compared to that of stoichimetric HAp consisting of globular particles [10]. These reports described that the response in terms of cellular behavior to HAp crystal was dependent on crystal size, morphology and types of cells. Thus, the morphological control of HAp is important for development of clinical and biological applications.

HAp synthesis has been carried out using several methods, such as solid-state reaction, wet chemical methods, gel growth methods and hydrothermal methods [11]. The hydrothermal method is the one most commonly used to prepare well-crystallized, single crystal HAp [12]. Thus many researchers have attempted to control the crystal size and/or morphology of HAp using hydrothermal methods [13–21]. The crystal growth and morphology of HAp significantly depend on the starting materials and hydrothermal conditions such as temperatures, treatment periods and additives to the aqueous solution.

In hydrothermal processing for fabrication of HAp, some organic molecules have been added to control morphology. Organic molecules affect the chemical reaction in a range of ways, such as via a chelating effect with calcium ions, pH increasing with molecular degradation, or molecular adsorption

* Corresponding author. Tel.: +81 0 52 789 3346; fax: +81 0 52 789 3182.
E-mail address: goto.tomoyo@c.mbox.nagoya-u.ac.jp (T. Goto).

0272-8842/$36.00
doi:10.1016/j.ceramint.2011.08.023

to crystal faces under hydrothermal conditions [13–21]. Calcium chelating agents, such as acetic acid, citric acid or ethylenediaminetetraacetic acid, have often been used to prevent the rapid calcium phosphate precipitation [15,16]. Functional groups on organic molecules, such as amino groups and carboxyl groups, also affect the morphology of the HAp crystals by a mechanism involving adsorption of the molecules on the surfaces of crystals during the crystal growth [17,18]. For instance, the effect of the hydroxyl group from alcohol on growth of HAp under hydrothermal conditions has been discussed. Nagata et al. reported that addition of methanol into the aqueous solution used for hydrothermal processing with HAp slurry as a precursor lead to formation of plate-shaped HAp [19]. Mizutani et al. reported that large-sized HAp whiskers were prepared by hydrothermal treatment of calcium tripolyphosphate gel using various alcohols [20]. In addition, Guo et al. reported the effect of isopropanol on the synthesis of HAp nanoparticles from low crystalline HAp under hydrothermal conditions [21]. These results show that alcohol was useful to control the morphology of HAp crystals formed in hydrothermal synthesis of HAp.

When low crystalline HAp was used as a starting material, the size of the final synthesized HAp was small [19,21]. On the other hand, large-sized HAp crystals were obtained using another starting material [20]. The crystal size of the product is affected by the crystal growth rate of HAp from the starting material. Thus we expect that large crystals of HAp can be produced by using starting materials with high reactivity with the surrounding solution, such as calcium orthophosphates. Application of water–ethanol solution gives a way to reduce the rate of dissolution of starting materials. The treatment using the water–ethanol solution is regarded as solvothermal processing [12]. However such a solvothermal treatment with water–ethanol solution and calcium orthophosphate as a starting material has not been studied for fabrication of HAp crystals. We expect that the solvothermal treatment of alpha-tricalcium phosphate (α-TCP) in water–ethanol solution will allow control of HAp formation, because the solubility of α-TCP is high [11] and it is easily transformed into HAp after reaction with water. The mixed water–ethanol solvent system should retard the reaction and cause slower crystal growth of HAp. In this study, the effects of the ethanol fraction in solution on the formation of HAp via solvothermal treatment of α-TCP were investigated. We used solutions with different ratios of ethanol to water. The changes in crystal phase, size, morphology and composition of the product as a function of the water:ethanol fraction were examined. In addition, the results are discussed in terms of the crystal growth mechanism of HAp from α-TCP in the water–ethanol system.

2. Materials and methods

2.1. Solvothermal treatment

α-TCP (Taihei Chemical Industrial Co., Ltd., Osaka, Japan) was hydrothermally treated in solutions with different proportions of water and ethanol (Nacalai Tesque, Inc., Kyoto, Japan), as given in Table 1. 0.25 g of α-TCP powder was placed in a 90 cm^3 vessel (Shikokurika Co., Ltd., Kochi, Japan), and then 20 cm^3 of the mixed solvent was added into the vessel. The vessels were sealed and kept at 120 °C for various periods ranging from 3–24 h after initial heating for 30 min to reach the treatment temperature. After the solvothermal treatment, the vessel was cooled to room temperature. The samples were removed from the vessel and then washed with ethanol and acetone to terminate any reaction. The samples were dried at 40 °C for at least 12 h.

Table 1
Sample notation and treatment conditions.

Notation	Volume/cm^3	
	Water	Ethanol
W20E00	20	0
W15E05	15	5
W10E10	10	10
W05E15	5	15
W00E20	0	20

2.2. Characterization

The phases of the samples were identified by powder X-ray diffraction (XRD; RINT2100HL, Rigaku Co., Tokyo, Japan) using CuKα radiation at 40 kV and 20 mA. The fractions (F) of HAp and other phases formed in the samples were evaluated semiquantitatively from the XRD patterns using the following formula:

$$F\,(\%) = \frac{I}{I_{\mathrm{HAp}} + I_{\alpha-\mathrm{TCP}} + I_{\beta-\mathrm{TCP}} + I_{\mathrm{DCPD}} + I_{\mathrm{DCPA}}} \times 100 \quad (1)$$

I_{HAp} is the integrated intensity of the HAp 211 reflection at $2\theta = 31.8^\circ$; $I_{\alpha\text{-TCP}}$, $I_{\beta\text{-TCP}}$, I_{DCPD}, and I_{DCPA} are the integrated intensities of the α-TCP 132 reflection at $2\theta = 24.1^\circ$, the beta-tricalcium phosphate (β-TCP) 214 reflection at $2\theta = 27.8^\circ$, the dicalcium phosphate dihydrate (DCPD) $12-1$ reflection at $2\theta = 20.9^\circ$ and the dicalcium phosphate anhydrous (DCPA) 002 reflection at $2\theta = 26.4^\circ$, respectively. In addition, I is the integrated intensity of the HAp, α-TCP, β-TCP and DCPA. The morphology of samples was observed by a scanning electron microscope (SEM; JSM-5600, JEOL Ltd., Tokyo, Japan). For SEM observation, a thin film of gold was sputtered onto the surfaces of the samples. Crystal size of the synthesized HAp was determined from the SEM images. The aspect ratio was calculated from the length and width of HAp crystals. The crystal growth rate was defined as the apparent crystal growth behavior using the following formula:

$$\text{Crystal growth rate} = \frac{dS}{dt} \quad (2)$$

where t is treatment period and S is crystal size (length or width) at that treatment period. A Fourier transform infrared spectrometer (FT-IR; FT/IR-610, JASCO Co., Tokyo, Japan) was

used to examine the structures of samples. The samples before and after the solvothermal treatment were ground and mixed with potassium bromide (KBr) at a mass ratio of about sample/KBr = 1/50. The mixed powder was then pressed into pellets for analysis in transmission mode. In addition, the Ca/P atomic ratio of the synthesized HAp crystal was measured using an inductively coupled plasma atomic emission spectrometer (ICP-AES; Optima 2000DV, PerkinElmer Japan Co., Ltd., Japan).

3. Results

3.1. Effects of ethanol addition on HAp formation

After the solvothermal treatment, the aggregation of powders was observed at the bottom of the vessel for samples W20E00, W15E05, W10E10 and W05E15 regardless of the treatment period. In contrast, the sample W00E20 was not aggregated even after solvothermal treatment for 24 h.

Fig. 1 shows powder XRD patterns of the samples before and after solvothermal treatment at 120 °C for (a) 3 h and (b) 24 h. The pattern from sample treated with just water for 3 h (W20E00) was assigned to only HAp (PDF No. 76-0694) phase. In contrast, the phase of the sample treated with just ethanol (W00E20) was not changed, remaining as α-TCP (PDF No. 70-0364) after treatment for 24 h. The samples with higher fractions of water in the mixed solution (W15E05) were assigned to only HAp phase after the treatment. With increasing fraction of ethanol (W10E10 and W05E15), formation of β-TCP (PDF No. 09-0169) and HAp was detected in the samples after treatment for 3 h. After treatment for 24 h, DCPA (PDF No. 77-0128) was detected in the samples prepared with high fractions of ethanol in the solution (W10E10 and W05E15). Comparing the XRD patterns of the samples treated for 24 h showed that the crystallinity of the HAp formed increased with increasing fraction of ethanol in the solution.

Fig. 2 shows the SEM images of the samples before and after solvothermal treatment at 120 °C for 24 h. Plate-like crystals 1–3 μm across were observed in the W20E00 sample after treatment. For W15E05, both plate-like and needle-like crystals were observed. The needle-like crystals were approximately 3 μm in length. In W10E10 and W05E15, only needle-like crystals were observed. The needle-like crystals from W10E10 appeared longer than those from W15E05. In contrast, the W00E20 treated in just ethanol shows similar morphology and size before and after the treatment.

Fig. 3 shows the relationships between the fractions of ethanol in the solution and crystal size and aspect ratio of precipitates observed after solvothermal treatment at 120 °C for 24 h. The aspect ratio was calculated from the length and width of crystals observed on the SEM images. For W00E20, the aspect ratio was not calculated because the formation of HAp was not observed. The crystal length increased with increasing fraction of ethanol (Fig. 3(a)). For the sample treated with only water (W20E00), the average crystal length was 2.1 μm. The average HAp crystal lengths were 3.3 and 4.6 μm in the samples treated with 25 (W15E05) or 50% (W10E10) fractions of ethanol, respectively. However, when the fraction of ethanol was over 50% in the mixed solvent (W05E15), the crystal length no longer increased (average crystal length was 4.0 μm). In contrast, the crystal width was decreased upon addition of ethanol to the solvent, changing from 1.1 μm (W20E00) to 0.3 μm (W15E05). The aspect ratio was somewhat increased with increasing fraction of ethanol in the mixed solvent

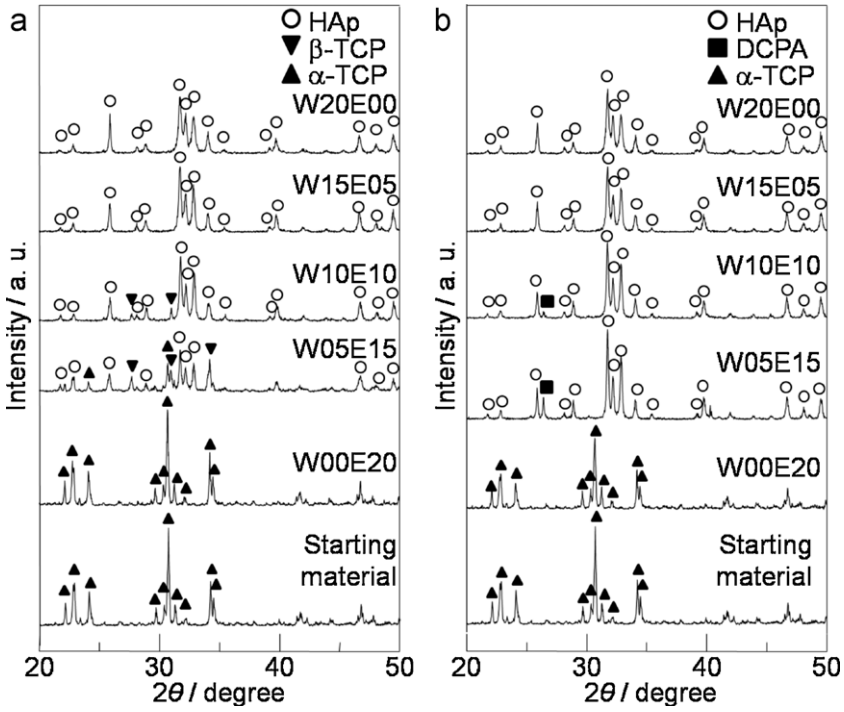

Fig. 1. XRD patterns of the α-TCP powder and samples after solvothermal treatment using water–ethanol solutions at 120 °C for (a) 3 h and (b) 24 h.

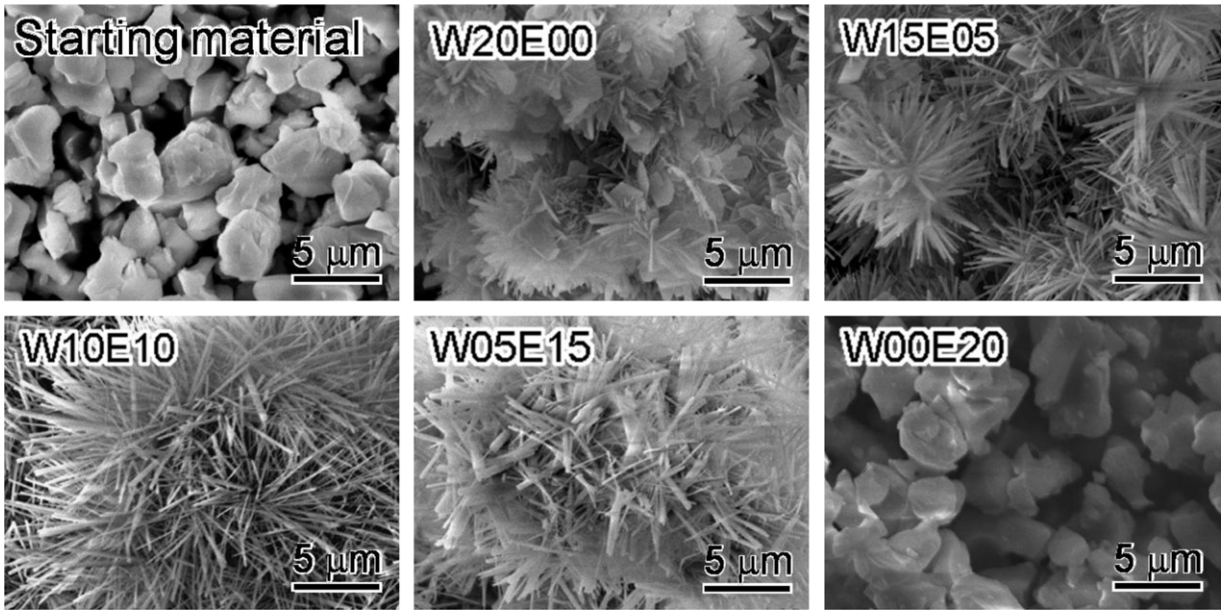

Fig. 2. SEM images of the α-TCP powder and samples after solvothermal treatment using water–ethanol solutions at 120 °C for 24 h.

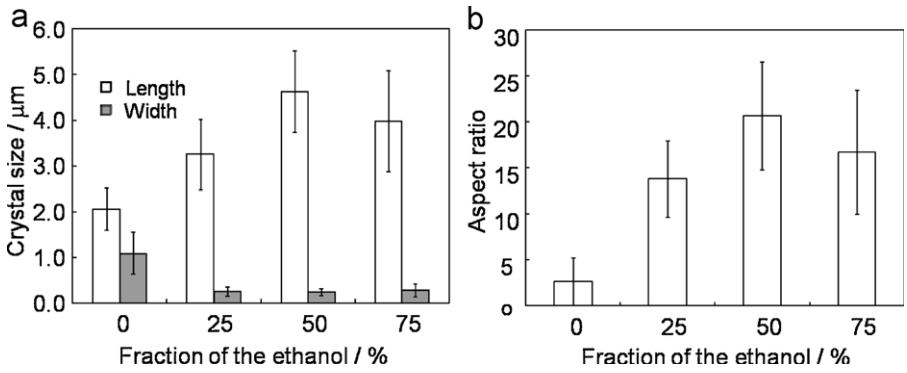

Fig. 3. Relationships between the ethanol fraction in the mixed solutions and crystal size and shape of products after solvothermal treatment at 120 °C for 24 h: (a) length and width and (b) aspect ratio.

(Fig. 3(b)). The change in aspect ratio with ethanol fraction showed a similar trend to the change in crystal length.

Fig. 4 shows the FT-IR spectra of the starting material (α-TCP) and the samples after solvothermal treatment at 120 °C for 24 h. The broad band at 3600−3000 cm^{-1} is assigned to adsorbed water molecules and the band at 1637 cm^{-1} is assigned to the bending mode of water. The bands at 1090, 1036 and 962 cm^{-1} are assigned to the P–O stretching vibration mode, and the bands at 604 and 565 cm^{-1} are assigned to the O–P–O bending mode of the phosphate group. The bands at 3571 and 633 cm^{-1} are assigned to the stretching and vibration modes of the hydroxyl group, respectively. In addition, the band at 868 cm^{-1} is assigned to the P–O(H) stretching mode of the HPO_4^{2-} group. From these results, all the samples except W00E20 show typical HAp spectra after solvothermal treatment [22]. The presence of the HPO_4^{2-} band shows that the HAp that has formed is HPO_4^{2-} substituted HAp crystal. The Ca/P atomic ratios for the HAp from the single phase samples (W20E00 and W15E05) after solvothermal treatment at 120 °C for 24 h are shown in Table 2. No significant difference in Ca/P atomic ratio of the HAp that formed was observed, with both HAp samples having Ca/P ≈ 1.5.

3.2. Treatment time-dependent change of HAp formation

Fig. 5 shows the *F* values, fractions of integrated intensity, for HAp, α-TCP, β-TCP and DCPA from the XRD patterns of (a) W20E00 and (b) W05E15 after solvothermal treatment at 120 °C for various periods. The W20E00 sample completely transformed into HAp after solvothermal treatment for 3 h (Fig. 5(a)). No α-TCP, β-TCP or DCPA was observed in this sample after solvothermal treatment. The rate of HAp

Table 2
Ca/P atomic ratio and morphology of formed HAp crystal.

	W20E00	W15E05
Morphology	Plate	Plate/Needle
Ca/P atomic ratio	1.54	1.51

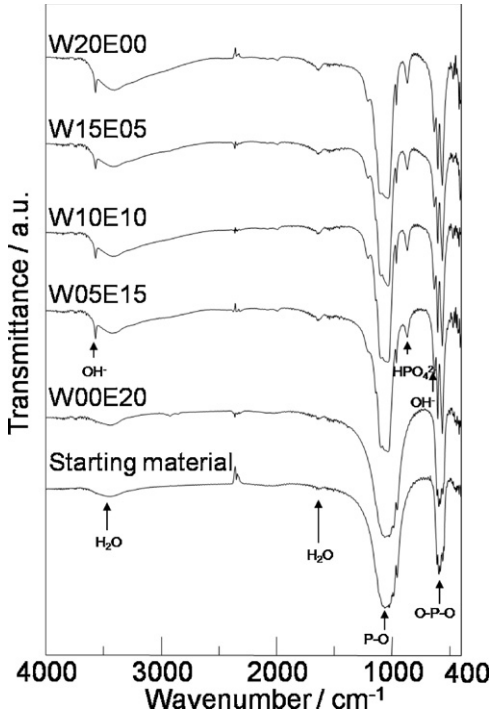

Fig. 4. FT-IR spectra of the α-TCP powder and samples after solvothermal treatment using either pure water or water–ethanol mixed solution at 120 °C for 24 h.

formation for sample W05E15 was lower than for W20E00 (Fig. 5(b)). In addition, W05E15 was only about 90% transformed into HAp even after 24 h. α-TCP and β-TCP were observed at the initial stages of the solvothermal treatment (3–12 h), and DCPA was formed at 12 h. The amount of DCPA increased with increasing treatment period.

Fig. 6 shows the change in crystal length and width per unit time after solvothermal treatment at 120 °C for various periods. These crystal sizes were calculated from the SEM images. Crystal length increased with increasing fraction of ethanol; however the crystal length was not changed by increasing treatment period (Fig. 6(a)). The widths were decreased by addition of ethanol (Fig. 6(b)), and no increase in width was observed upon increasing treatment period (in contrast to the trend for crystal length).

Fig. 7 shows the change in crystal growth rate calculated from the crystal length and width per unit time after solvothermal treatment at 120 °C for various periods. Here the crystal growth rate at the initial stage of the solvothermal treatment, calculated from the change in crystal size from 0 h to 3 h was shown as the value at 0 h. The change in the lengthwise crystal growth rate decreased with increasing treatment period (Fig. 7(a)). The lengthwise crystal growth rate of W20E00 was the lowest of all the samples at the early stage (for 0 h). In contrast, the W20E00 sample displayed the highest widthwise crystal growth rate of all the samples at the early stage (for 0–6 h) (Fig. 7(b)). Both widthwise and lengthwise crystal growth

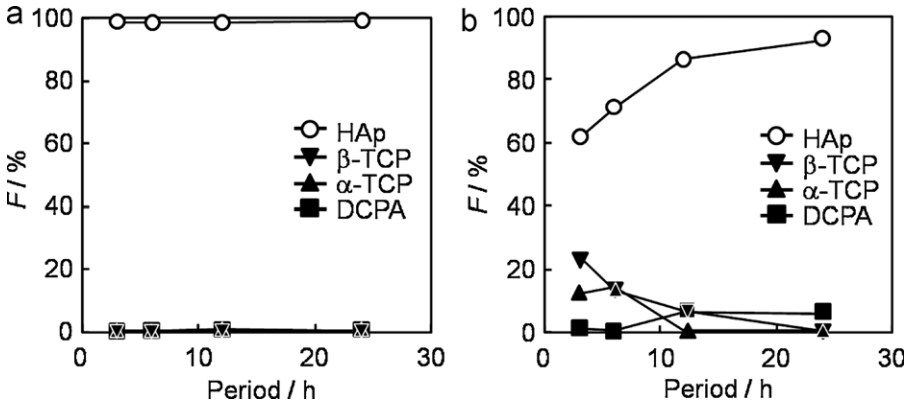

Fig. 5. *F*, the fraction of integrated intensity from the XRD patterns, for HAp, α-TCP, β-TCP and DCPA, in samples (a) W20E00 and (b) W05E15 after solvothermal treatment at 120 °C for various periods.

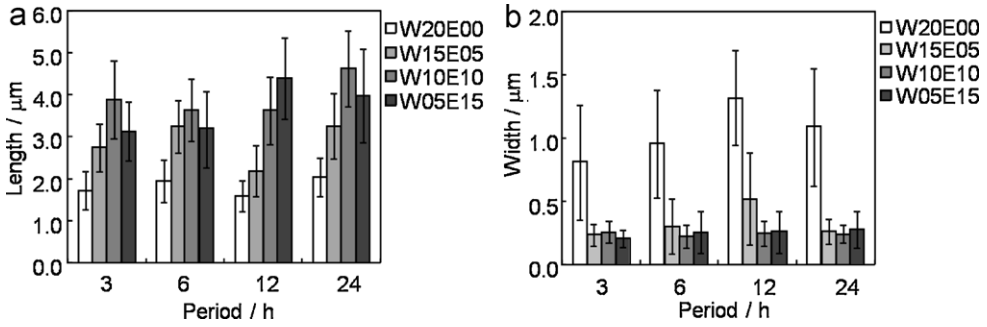

Fig. 6. Variation in crystal size and shape of products as a function of treatment period: (a) length and (b) width.

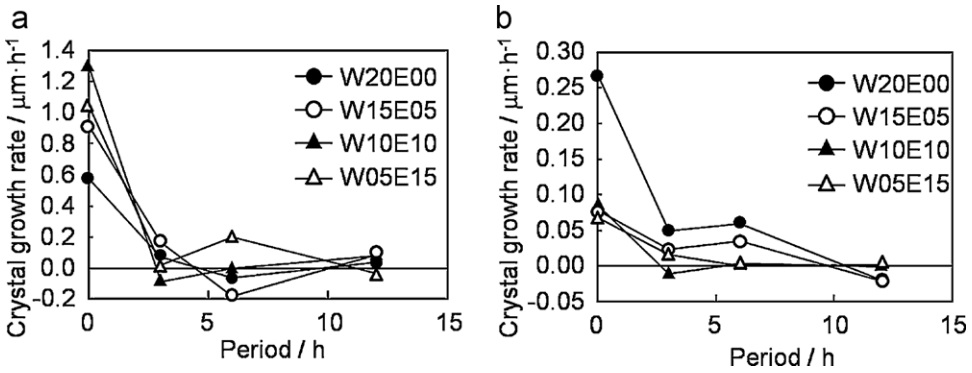

Fig. 7. Change in the crystal growth rate as a function of treatment period: (a) length and (b) width.

rates became closer to 0 μm/h as the period of the solvothermal treatment increased.

4. Discussion

The XRD patterns confirmed that the transformation from α-TCP into HAp was inhibited with increasing fraction of ethanol. When α-TCP was treated with pure ethanol, α-TCP was not transformed into HAp. This was because sufficient water is required for the reaction of HAp as shown in the following formula:

$$10Ca_3(PO_4)_2 + 6H_2O \rightarrow 3Ca_{10}(PO_4)_6(OH)_2 + 2PO_4^{3-} + 6H^+ \quad (3)$$

A previous study reported that the rate of transformation of α-TCP into HAp in the water–ethanol system was lower than that in the water system in conventional wet processing [23]. The present transformation rate trend for water–ethanol solution under solvothermal conditions is consistent with this previous report.

Note that β-TCP was formed in the W10E10 and W05E15 samples. The higher fraction of ethanol in the solution leads to formation of β-TCP prior to HAp formation. β-TCP may be formed as a metastable phase by dissolution–precipitation processes under the solvothermal conditions used in this study. At high fraction of ethanol in the solvent, β-TCP was observed, accompanied by a decrease in the formation rate of HAp. Ca^{2+} and PO_4^{3-} ions in the mixed solvent react with hydroxide ions with difficulty, so the stabilized phase β-TCP precipitates at the low temperature instead. DCPA as a by-product was also formed in samples W10E10 and W05E15 after 24 h (Fig. 1(b)). The F of DCPA in W05E15 (Fig. 5(b)) increased with increasing treatment period. These results show that HAp formation was inhibited, and DCPA formation increased with increasing fraction of ethanol in the solvent. It was reported that, based on the solubility isotherms of calcium phosphate phases, the solubility of DCPA is lower than that of HAp under acidic conditions [11]. In addition, HAp formation from α-TCP leads to pH decrease (formula (3)). Therefore, from the DCPA formation, we suggest that the decrease of pH value of the solvent was enhanced with increasing treatment period in mixed solvents with a high proportion of ethanol. In other words, in the case of the solution with the high proportion of ethanol (W05E15), DCPA formation from α-TCP is enhanced by the increasing amount of H^+ in water–ethanol solution as shown in the following reactions:

$$Ca_3(PO_4)_2 \rightarrow 3Ca^{2+} + 2PO_4^{3-} \quad (4)$$

$$PO_4^{3-} + H^+ \rightarrow HPO_4^{2-} \quad (5)$$

$$Ca^{2+} + HPO_4^{2-} \rightarrow CaHPO_4 \quad (6)$$

The Ca/P ratio of the HAp formed was 1.5 (from the ICP-AES measurement), and the FT-IR spectra show that the HAp was substituted. This Ca/P ratio is lower than that of stoichiometric HAp (Ca/P = 1.67). It would appear that HPO_4^{2-} is easily substituted into the HAp crystal because the Ca/P atomic ratio of α-TCP is 1.5. In the present study, the Ca/P atomic ratio and composition was not affected by ethanol addition.

The morphology of the HAp crystal changed from plate-shaped to needle-shaped with increasing fraction of ethanol in the solution. The change of crystal morphology was not affected by the treatment period. In addition, the aspect ratio of the needle-like HAp crystals increased with increasing ethanol fraction in the solution. It was reported that addition of ethanol to aqueous solution may reduce the dissolved amounts of Ca^{2+} and PO_4^{3-} in the solution, and lead to more rapid precipitation of calcium phosphate such as HAp [24,25]. In addition, Tung et al. reported that the solubility of HAp decreased upon ethanol addition [26]. The dielectric constants of water and ethanol at 25 °C are 78.5 and 24.3, respectively, meaning that the dielectric constant of water–ethanol solution will decrease with increasing ethanol fraction. Thus the change of crystal morphology is attributable not only to the supply rate of water for the hydration of α-TCP, but also to the change in the solubility of α-TCP and HAp. The amounts of dissolved α-TCP in the mixed solution are likely to be less than in the pure water. Therefore, the decreased amount of dissolved ions from α-TCP may result in a decrease in the HAp formation rate. The size of the HAp crystals will increase with decreasing HAp formation rate, because HAp nucleation will be dominant over crystal growth under conditions of saturation with respect to HAp. This

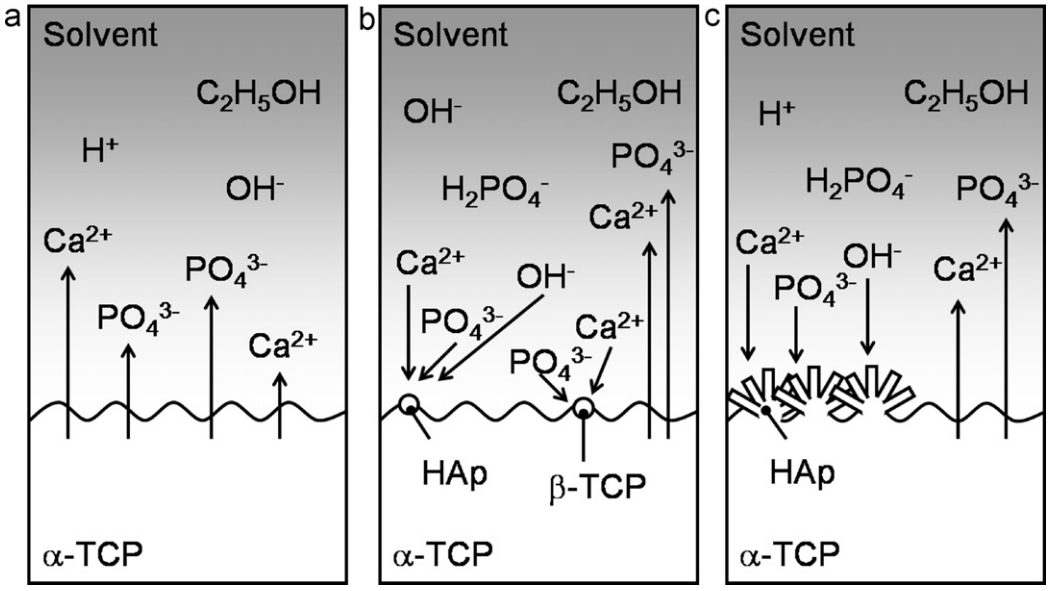

Fig. 8. Schematic illustration of the mechanism for needle-like HAp formation in the water–ethanol mixed solvent under solvothermal conditions: (a) dissolution of α-TCP, (b) nucleation of HAp and β-TCP and (c) crystal growth of needle-like HAp.

relation between alcohol amount and aspect ratio was consistent with previous reports [20,21]. In general, for HAp formation, the crystal morphology adopts the equilibrium form when the crystal growth rate is slow. Suzuki et al. reported that the *a*-face (10 − 10) of chlorapatite crystal is more stable than *c*-face (10 − 11) based on the specific surface free energies calculated from contact angles [27,28]. Therefore, with increasing ethanol fraction in the solution, it would appear that the crystal morphology of HAp became rod-shaped, which exposed *a*-face (the equilibrium form). In the case of this study, which used a highly soluble material, α-TCP, compared to other calcium phosphates, a remarkable change in crystal morphology was observed. Thus, these results mean that the morphology and size of HAp can be controlled when using α-TCP by the ethanol fraction in the solution under solvothermal conditions.

Fig. 8 shows the crystal growth mechanism of HAp from α-TCP in water and ethanol mixed solvents under solvothermal conditions. First, Ca^{2+} and PO_4^{3-} ions were dissolved from α-TCP (Fig. 8(a)). The amount of dissolved Ca^{2+} and PO_4^{3-} ions in the mixed solvent is smaller than that in the pure water. In addition, PO_4^{3-} ion becomes $H_2PO_4^-$ or HPO_4^{2-} ion when the solution pH is neutral. In other words, the pH will be increased, as the OH^- concentration also increases. Therefore, it would appear that the degree of supersaturation with respect to HAp in mixed solvent is high. In the supersaturated solution, growth units are generally formed, such as the $Ca_9(PO_4)_6$ ''Posner cluster'' for crystal growth of HAp [29]. Onuma et al. reported that calcium phosphate clusters exist in fluid supersaturated with respect to HAp [30]. Consequently, it is possible that calcium phosphate clusters for the growth of HAp crystals were formed in the water–ethanol system under the solvothermal conditions. However, formation of calcium phosphate cluster is not depicted in schematic illustration of Fig. 8, and in this study, elementary species such as ions and molecules were used for the sake of simplicity when considering the growth mechanism. It was estimated that the amount of nucleation in the mixed solution was lower than for the pure water condition. The HAp nucleation occurred on the α-TCP powder (Fig. 8(b)). At the same time, some Ca^{2+} and PO_4^{3-} ions were re-precipitated as β-TCP because β-TCP is more stable than α-TCP under this condition. Third, crystal HAp keeps growing by consuming the surrounding Ca^{2+} and PO_4^{3-} ions (Fig. 8(c)). The crystal growth of HAp is slow in the mixed solution because the dissolution rate of α-TCP is slow. In addition, the morphology of the HAp crystal became needle-shaped with increasing ethanol fraction in the mixed solvent. Fig. 7 suggests that the crystal growth of HAp has reached an apparent equilibrium after solvothermal treatment for over 12 h.

The present study was focused mainly on changes in morphology of HAp crystal through solvothermal treatment of α-TCP in water–ethanol system. This technique can be applied to morphological control of ceramic biomaterials for artificial bone and their coating on bone repairing biomaterials. Actually, previous reports indicated that crystal morphology of HAp affected the protein adsorption [9,31,32] and biological behavior [8–10]. Thus our results would be helpful to develop novel artificial bones designed not only from composition and porosity, but also from morphology and crystal plane of HAp.

5. Conclusions

We investigated the effect of ethanol fraction on solvothermal synthesis of HAp from α-TCP as a starting material. With increasing fraction of ethanol in the solutions, the rate of transformation into HAp was decreased. β-TCP and DCPA by-products were observed in the samples with high proportion of ethanol in mixed solvent. The morphology of HAp crystal was changed from plate-shaped to needle-shaped with increasing ethanol fraction. In addition, the aspect ratio of HAp crystal was

increased with increasing fraction of ethanol. The rate of crystal growth and the morphology of HAp were controlled by the ethanol addition in the solvothermal synthesis from α-TCP as a starting material.

Acknowledgements

The authors appreciate support from the G-COE program (Global Center of Excellence Program, Japan Society for the Promotion of Science). This work was partially supported by a Grant-in-Aid for Scientific Research on Innovative Areas, ''Fusion Materials: Creative Development of Materials and Exploration of Their Function through Molecular Control'' (no. 2206) from the Ministry of Education, Culture, Sports, Science and Technology, Japan (MEXT).

References

[1] J. Park, Bioceramics: Properties, Characterizations and Applications, Springer, New York, 1998.
[2] A. Tiselius, S. Hjertén, Ő. Levin, Protein chromatography on calcium phosphate columns, Arch. Biochem. Biophys. 65 (1956) 132–155.
[3] G. Bernardi, Chromatography of nucleic acids on hydroxyapatite, Nature 206 (1965) 779–783.
[4] T. Kawasaki, S. Takahashi, K. Ikeda, Hydroxyapatite high-performance liquid chromatography: column performance for proteins, Eur. J. Biochem. 152 (1985) 361–371.
[5] T. Kawasaki, K. Ikeda, S. Takahashi, Y. Kuboki, Further study of hydroxyapatite high-performance liquid chromatography using both proteins and nucleic acids, and a new technique to increase chromatographic efficiency, Eur. J. Biochem. 155 (1986) 249–257.
[6] Y. Shinto, A. Uchoda, F. Korkusuz, N. Araki, K. Ono, Calcium hydroxyapatite ceramic used as a delivery system for antibiotics, J. Bone Joint Surg. Br. 74B (1992) 600–604.
[7] B.J. Melde, A. Stein, Periodic macroporous hydroxyapatite-containing calcium phosphates, Chem. Mater. 14 (2002) 3326–3331.
[8] S. Okada, H. Ito, A. Nagai, J. Komotori, H. Imai, Adhesion of osteoblast-like cells on nanostructured hydroxyapatite, Acta Biomater. 6 (2010) 591–597.
[9] S. Okada, A. Nagai, Y. Oaki, J. Komotori, H. Imai, Control of cellular activity of fibroblasts on size-tuned fibrous hydroxyapatite nanocrystals, Acta Biomater. 7 (2011) 1290–1297.
[10] T. Okuda, K. Ioku, I. Yonezawa, H. Minagi, Y. Gonda, G. Kawachi, M. Kamitakahara, Y. Shibata, H. Murayama, H. Kurosawa, T. Ikeda, The slow resorption with replacement by bone of a hydrothermally synthesized pure calcium-deficient hydroxyapatite, Biomaterials 29 (2008) 2719–2728.
[11] J.C. Elliot, Structure and Chemistry of the Apatites and Other Calcium Orthophosphates, Elsevier, Amsterdam, 1994.
[12] M. Yoshimura, H. Suda, Hydrothermal processing of hydroxyapatite: past, present, and future, in: P.W. Brown, B. Constantz (Eds.), Hydroxyapatite and Related Materials, CRC Press, Boca Raton, 1994, pp. 45–72.
[13] C.M. Zhang, J. Yang, Z.W. Quan, P.P. Yang, C.X. Li, Z.Y. Hou, J. Lin, Hydroxyapatite nano- and microcrystals with multiform morphologies: controllable synthesis and luminescence properties, Cryst. Growth Des. 9 (2009) 2725–2733.
[14] I.S. Neira, Y.V. Kolen'ko, O.I. Lebedev, G. Van Tendeloo, H.S. Gupta, F. Guitián, M. Yoshimura, An effective morphology control of hydroxyapatite crystals via hydrothermal synthesis, Cryst. Growth Des. 9 (2009) 466–474.
[15] M. Yoshimura, H. Suda, K. Okamoto, K. Ioku, Hydrothermal synthesis of biocompatible whiskers, J. Mater. Sci. 29 (1994) 3399–3402.
[16] Y. Fujishiro, H. Yabuki, K. Kawamura, T. Sato, A. Okuwaki, Preparation of needle-like hydroxyapatite by homogeneous precipitation under hydrothermal conditions, J. Chem. Technol. Biotechnol. 57 (1993) 349–353.
[17] F. Nagata, M. Toriyama, K. Teraoka, Y. Yokogawa, Influence of ethylamine on the crystal growth of hydroxyapatite crystals, Chem. Lett. 30 (2001) 780–781.
[18] T. Toyama, A. Oshima, T. Yasue, Hydrothermal synthesis of hydroxyapatite whisker from amorphous calcium phosphate and the effect of carboxylic acid, J. Ceram. Soc. Jpn. 109 (2001) 232–237 (In Japanese).
[19] F. Nagata, Y. Yokogawa, M. Toriyama, Y. Kawamoto, T. Suzuki, K. Nishizawa, Hydrothermal synthesis of hydroxyapatite crystals in the presence of methanol, J. Ceram. Soc. Jpn. 103 (1995) 70–73 (In Japanese).
[20] Y. Mizutani, M. Hattori, M. Okuyama, T. Kasuga, M. Nogami, Large-sized hydroxyapatite whiskers derived from calcium tripolyphosphate gel, J. Eur. Ceram. Soc. 25 (2005) 3181–3185.
[21] X. Guo, P. Xiao, Fffects of solvents on properties of nanocrystalline hydroxyapatite produced from hydrothermal process, J. Eur. Ceram. Soc. 26 (2006) 3383–3391.
[22] S. Koutsopoulos, Synthesis and characterization of hydroxyapatite crystals: a review study on the analytical methods, J. Biomed. Mater. Res. 62 (2002) 600–612.
[23] A. Nakahira, K. Sakamoto, S. Yamaguchi, M. Kaneno, S. Takeda, M. Okazaki, Novel synthesis method of hydroxyapatite whiskers by hydrolysis of α-tricalcium phosphate in mixtures of water and organic solvent, J. Am. Ceram. Soc. 82 (1999) 2029–2032.
[24] M.J. Larsen, A. Thorsen, S.J. Jensen, Ethanol-induced formation of solid calcium phosphates, Calcif. Tissue Int. 37 (1985) 189–193.
[25] E. Lerner, R. Azoury, S. Sarig, Rapid precipitation of apatite from ethanol-water solution, J. Cryst. Growth 97 (1989) 725–730.
[26] M.S. Tung, C. Lin, T.H. Chow, P. Sung, The effect of ethanol on the solubility of hydroxyapatite in the system $Ca(OH)_2$–H_3PO_4–H_2O at 25° and 33 °C, in: P.W. Brown, B. Constantz (Eds.), Hydroxyapatite and Related Materials, CRC Press, Boca Raton, 1994, , pp.145–151.
[27] T. Suzuki, G. Hirose, S. Oishi, Contact angle of water droplet on apatite single crystals, Mater. Res. Bull. 39 (2004) 103–108.
[28] T. Suzuki, I. Kumeda, K. Teshima, S. Oishi, Specific surface free energies of strontium chlorapatite single crystal determined by contact angles of liquid droplets, Chem. Phys. Lett. 421 (2006) 343–347.
[29] A.S. Posner, F. Betts, Synthetic amorphous calcium phosphate and its relation to bone mineral structure, Acc. Chem. Res. 8 (1975) 273–281.
[30] K. Onuma, A. Ito, Cluster growth model for hydroxyapatite, Chem. Mater. 10 (1998) 3346–3351.
[31] T. Akazawa, M. Kobayashi, T. Kanno, K. Kodaira, Characterization of albumin- and lysozyme-adsorption evaluated on two differently prepared apatites, J. Mater. Sci. 33 (1998) 1927–1931.
[32] G. Kawachi, T. Watanabe, S. Ogata, M. Kamitakahara, C. Ohtsuki, Protein adsorption on needle-shaped hydroxyapatite prepared by hydrothermal treatment of mixture composed of $CaHPO_4{\cdot}2H_2O$ and β-$Ca_3(PO_4)_2$, J. Ceram. Soc. Jpn. 117 (2009) 847–850.